

Negligible voltage hysteresis with strong anionic redox in conventional battery electrode



Kehua Dai ^{a,b,c,*}, Jing Mao ^d, Zengqing Zhuo ^{c,e}, Yan Feng ^a, Wenfeng Mao ^a, Guo Ai ^f, Feng Pan ^e, Yi-de Chuang ^c, Gao Liu ^{g, **}, Wanli Yang ^{c, ***}

^a College of Chemistry, Tianjin Normal University, Tianjin, 300387, China

^b School of Metallurgy, Northeastern University, Shenyang, 110819, China

^c Advanced Light Source, Lawrence Berkeley National Laboratory, Berkeley, CA, 94720, United States

^d School of Materials Science and Engineering, Zhengzhou University, Zhengzhou, 450001, China

^e School of Advanced Materials, Peking University Shenzhen Graduate School, Shenzhen, 518055, China

^f College of Physics and Materials Science, Tianjin Normal University, Tianjin, 300387, China

^g Energy Storage and Distributed Resources Division, Energy Technologies Area, Lawrence Berkeley National Laboratory, Berkeley, CA, 94720, United States

ARTICLE INFO

Keywords:

Oxygen redox
Sodium-ion batteries
Cathode materials
Synchrotron
Mapping of resonant inelastic X-ray scattering (mRIXS)

ABSTRACT

Lattice anionic (oxygen) redox reactions (ARR) offers opportunities for developing high-capacity batteries, however, often suffers the notoriously high hysteresis in voltages and low initial coulombic efficiency. Particularly, ARR was widely considered inherent to these kinetic issues. In this paper, unambiguous evidences of strong and reversible ARR is found in $\text{Na}_{2/3}\text{Ni}_{1/3}\text{Mn}_{2/3}\text{O}_2$ through mapping of resonant inelastic X-ray scattering (mRIXS). Strikingly, the material displays negligible voltage hysteresis (0.1 V) and high initial coulombic efficiency with a highly stable electrochemical profile. Our independent analysis of the Ni, Mn and O states consistently interpret the redox mechanism of $\text{Na}_{2/3}\text{Ni}_{1/3}\text{Mn}_{2/3}\text{O}_2$, which reveals a strong ARR system with facile kinetics and highly stable electrochemical profile that previously found only in cationic redox systems of conventional non-Alkali-rich materials.

1. Introduction

Anionic redox reactions (ARR) has attracted extensive attention because they offer opportunities to significantly improve the specific capacity of cathode materials in batteries [1–4]. However, the anionic redox in oxide electrodes, i.e., oxygen redox reactions [5], seems inherent to many performance issues [2,6], among which, strong voltage hysteresis [7–9] and low Coulombic efficiency [10] are broadly observed and widely associated with ARR [2,3,11]. This not only reduces energy density, but also greatly decreases energy storage efficiency, which becomes a fatal problem for its practicality. Indeed, a recent review by Assat and Tarascon pointed out that the voltage hysteresis and the sluggish kinetics are the most important practical issues for utilizing ARR, and the fundamental understanding of the association between them remains missing [2].

There are several interesting systems that provide direct indications

on the intriguing relationship between the ARR and voltage hysteresis. Firstly, the most studied ARR systems are the Li-rich compounds that include mostly 3d transition-metal (TM) oxides [1,2,12,13], but have been extended to 4d/5d TMs [14–17]. Voltage hysteresis problem is almost universal in these compounds. The only exception is Li_2IrO_3 , which displays highly reversible electrochemical profile with very low voltage hysteresis [14]. However, later studies clarified that Li_2IrO_3 itself does not have ARR unless doped with Sn, and voltage hysteresis unfortunately gets strong while ARR emerges in the Sn doped Li_2IrO_3 systems [18].

Secondly, very recent reports have revealed that non-Li-rich conventional layered compounds display ARR at high voltages too [19–22]. These findings benefit from recent advances of O-K high-efficiency mapping of resonant inelastic X-ray scattering (mRIXS), which could reliably detect the lattice (non-released) ARR in battery electrodes at charged states [23]. Other conventional Na-ion materials were also

* Corresponding author. College of Chemistry, Tianjin Normal University, Tianjin, 300387, China.

** Corresponding author.

*** Corresponding author.

E-mail addresses: daikehua@gmail.com (K. Dai), gliu@lbl.gov (G. Liu), wlyang@lbl.gov (W. Yang).

found to feature strong ARR [24,25], but the Mg dopants are highly ionic and actually mimic the chemical environment to oxygen as alkali metals, i.e., the case alike Li-rich compounds. Anyway, although all these non-alkali-rich compounds with ARR display generally improved voltage hysteresis behaviors compared with Li-rich compounds, the ARR itself takes place at high voltages, which often leads to strong voltage hysteresis and highly irreversible reactions [19–21].

Thirdly, several Na-ion battery cathode materials were reported with very low voltage hysteresis. For example, $\text{Na}_2\text{Mn}_3\text{O}_7$ displays a low voltage hysteresis of only about 50 mV [26,27], and $\text{Na}_{0.6}[\text{Li}_{0.2}\text{Mn}_{0.8}]\text{O}_2$ shows a 0.2 V voltage hysteresis, which are significantly lower than those of Li-ion compounds [28,29]. Both systems, however, display low Coulombic efficiency during initial cycles. Strikingly, P2-type $\text{Na}_{2/3}\text{Ni}_{1/3}\text{Mn}_{2/3}\text{O}_2$ (NNMO) not only displays a very low voltage hysteresis of only about 0.1 V [30–32], it also shows a highly reversible electrochemical profile with well-defined plateaus close to each other upon its charge and discharge process, leading to a high Coulombic efficiency during the initial cycle (Fig. 1a). Additionally, this material is highly air stable with great practical potentials [33], as well as excellent rate performance indicating facile kinetics [34]. The critical question here is whether the highly stable and high-rate properties stems from the typical cationic redox mechanism, or ARR could also offer such a good electrochemical performance with facile kinetics.

The debate on whether the NNMO is an ARR system has been going back and forth in previous literature [26,31,35–38]. Early works considered the stoichiometry and expected that the reaction mechanism is dominated by $\text{Ni}^{2+/4+}$ redox reactions, because the Ni redox with double electron transfer could compensate all the desodiation of $\text{Na}_{2/3}\text{Ni}_{1/3}\text{Mn}_{2/3}\text{O}_2$ [26,31,37,38]. However, recent report by Risthaus

et al. claimed signs of ARR in NNMO based on XAS analysis [35]. Note that the used O-K XAS pre-edge feature is dominated by the TM-3d states through TM-O hybridization that often does not represent oxygen redox states [39]. Indeed, such a conclusion was challenged by Cheng et al., who concluded that no ARR was found in the NNMO based on their RIXS observations [36]. However, this latest work also showed a strange finding on the Ni oxidation states, which remains very low throughout the cycling, indicating that the charged electrodes were somehow not fully oxidized in the study and contradicting other works with strong $\text{Ni}^{2+/4+}$ redox signatures [31,38]. Therefore, the redox mechanism of NNMO remains an open and important question. Clarifying the redox mechanism, especially the ARR, in NNMO system thus becomes a critical topic because it may finally confirm an ARR system without the kinetics issues in a commercially viable 3d TM based conventional electrode system for the first time.

In this work, we have carefully examined a series of NNMO electrodes with different SOC through electrochemically cycling. Each electrode was re-checked on their potential before experiments to make sure their charged states were sustained (see the experimental section). We performed a comprehensive experimental study and analysis of both the cationic redox activities, i.e., the evolution of Ni and Mn valence states [40–43], and the ARR activities through O-K mRIXS [24,44,45]. Our results show quantitatively, self-consistently, and unambiguously that NNMO system is a strong ARR system with negligible voltage hysteresis and high initial cycle Coulombic efficiency. We note that this is the first-time clear evidences of strong ARR are found in a non-alkali-rich system with highly reversible electrochemical profile even at the high voltage (ARR) range.

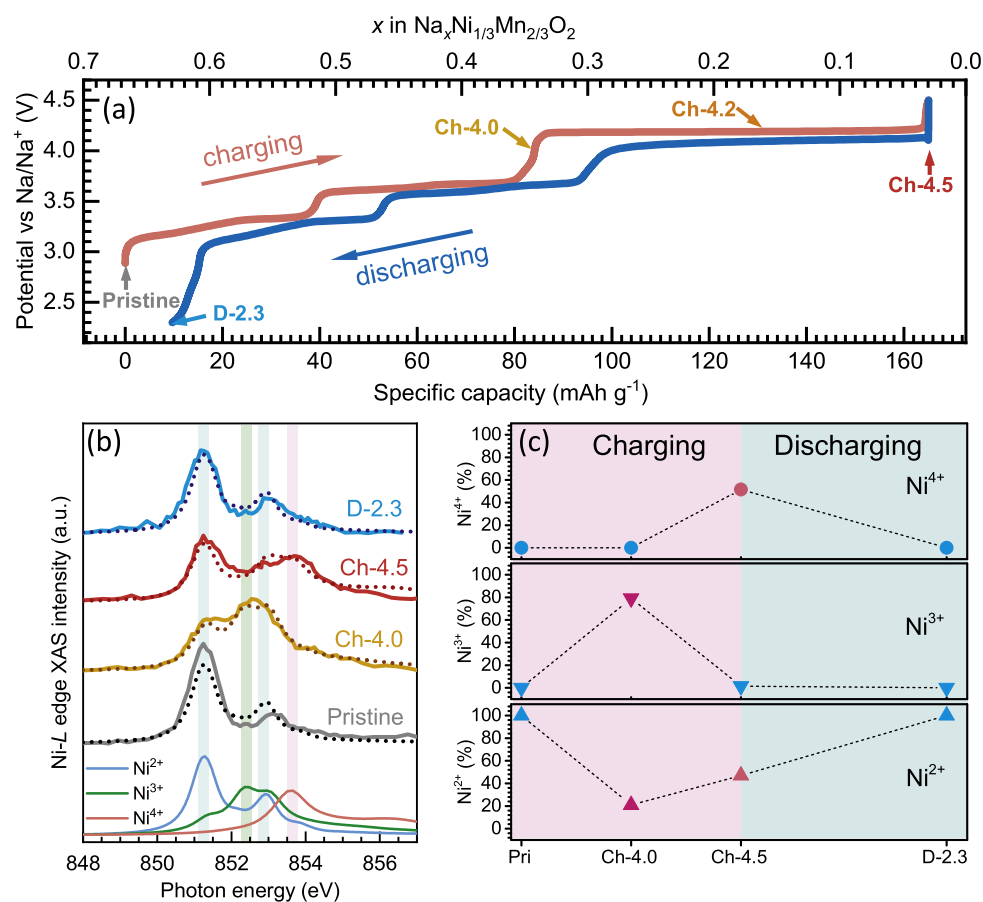


Fig. 1. The voltage profiles and the Ni, Mn valence evolutions. (a) The charging and discharging profiles of $\text{Na}_{2/3}\text{Ni}_{1/3}\text{Mn}_{2/3}\text{O}_2$ at 0.1C ($1\text{C} = 160 \text{ mA g}^{-1}$). (b) The Ni-L_3 edge TFY (solid) and fitted curves (dotted). (c) The Ni valence evolution upon electrochemical potentials.

2. Experimental

2.1. Materials preparation

$\text{Na}_{2/3}\text{Ni}_{1/3}\text{Mn}_{2/3}\text{O}_2$ was prepared by PVP-combustion method. Stoichiometric $\text{NaOAc}\cdot 4\text{H}_2\text{O}$, $\text{Ni}(\text{OAc})_2\cdot 4\text{H}_2\text{O}$ and $\text{Mn}(\text{OAc})_2\cdot 4\text{H}_2\text{O}$, and PVP (the molar ratio of PVP monomer to total metal ions was 2.0) were dissolved in deionized water and $\text{pH} = 3$ was achieved by adding 1:1 HNO_3 . The mixture was stirred at 120°C to obtain dried gel. The dried gel was ignited on a hot plate to induce a combustion process which lasted for several minutes. The resulting precursor was preheated at 400°C for 2 h and then calcined at 1000°C for 6 h with the heating rate of 5°C min^{-1} . After heat treatment, the oven was switched off and the sample was cooled down naturally. The whole process was performed in air.

2.2. Preparation of the characterized samples

The $\text{Na}_{2/3}\text{Ni}_{1/3}\text{Mn}_{2/3}\text{O}_2$ cathode was prepared by mixing 80 wt% active material, 10 wt% acetylene black (AB) and 10 wt% polyvinylidene fluoride (PVdF) binder in N-methylpyrrolidone (NMP) to form a slurry. The slurry was doctor-bladed onto aluminum foil, dried at 60°C , and then punched into electrode discs with a diameter of 12.7 mm. The prepared electrodes were dried at 130°C for 12 h in a vacuum oven and show typically an active material loading of about 4 mg cm^{-2} . Swagelok cells were fabricated with the $\text{Na}_{2/3}\text{Ni}_{1/3}\text{Mn}_{2/3}\text{O}_2$ cathode, sodium foil anode, 1 mol L^{-1} NaClO_4 in propylene carbonate (PC) as electrolyte, and double layered glass fiber as separator in an argon-filled glove box.

The cells were electrochemically cycled to the representative SOC at 0.1C rate, and then rested for 4 h to approach the open circuit potential (OCV). The cells were disassembled, and the electrodes were cut to two parts. One part was reassembled in the same Swagelok cell and its OCV was tested to ensure the electrode free of shortening. Another part was rinsed immediately with DMC thoroughly to lock the SOC and remove surface residue and then was vacuum dried at room temperature. The obtained electrodes were then loaded into our special sample transfer chamber inside the Ar-filled glove box. The sample transfer chamber was sealed, mounted onto the loadlock of XAS endstation for direct pump-down to avoid any air exposure effects.

2.3. X-ray absorption spectroscopy (XAS)

Soft x-ray absorption spectroscopy was performed in the iRIXS endstation at Beamline 8.0.1 of the Advanced Light Source (ALS) at LBNL [46]. XAS data are collected from the side of the electrodes facing current collector in both TEY and TFY modes. All the soft XAS spectra have been normalized to the beam flux measured by the upstream gold mesh. The experimental energy resolution is 0.15 eV without considering core-hole lifetime broadening.

2.4. Mapping of Resonant inelastic X-ray Scattering (mRIXS)

mRIXS measurements were performed in iRIXS endstation at Beamline 8.0.1 of the ALS [46]. Data were collected through the ultra-high efficiency modular spectrometer [47]. The resolution of the excitation energy is about 0.35 eV, and the emission energy about 0.25 eV. An excitation energy step size of 0.2 eV was chosen for all the maps. mRIXS were collected at each excitation energies. Final 2D images are obtained through a data process involving normalization to the beam flux and collection time, integration and combination, which has been detailed previously [48].

3. Results

Fig. 1a shows the initial voltage profile of NNMO at 0.1C . Sample

preparation and electrochemical profile have been discussed in previous works [34]. It is very important to note that the NNMO displays excellent rate capability and cycling stability with highly reversible charge-discharge profile, indicating decent kinetics in NNMO system [34]. The voltage hysteresis of 4.2-V plateau is only about 0.1 V at 0.1C (16 mA g^{-1}), which is comparable with traditional cathode materials, e.g. LiCoO_2 [21]. Studied samples are indicated in Fig. 1a as the pristine, Ch-4.0, Ch-4.2, Ch-4.5 and D-2.3.

The Ni redox reaction could be quantitatively analyzed by fitting the Ni-L TFY spectra using a linear combination of the $\text{Ni}^{2+}/\text{Ni}^{3+}/\text{Ni}^{4+}$ standard TFY spectra from calculations [41]. Fig. 1b shows the Ni-L₃ XAS spectra in TFY mode and the fitted curves. The fitted curves are in good agreement with the spectra, and the relative error of constant valence components is less than 5% (Table S1). Fig. 1c shows the Ni valence distribution at different charge/discharge states. From pristine to Ch-4.0, 80% of Ni^{2+} is oxidized to Ni^{3+} , as expected. Strikingly, charging the electrode from 4.0 to 4.5 V leads to a significant drop of Ni^{3+} and increase of Ni^{2+} contents, which is directly indicated by the strong lineshape change between the Ch-4.5 and Ch-4.0 spectra in both the TEY (Fig. S1) and TFY (Fig. 1b) results. Such a counterintuitive increase of Ni^{2+} at high voltage state provides the experimental evidence of the reductive coupling mechanism, which is also found in some ARR systems including LiNiO_2 [19,49–51]. However, the lineshape change here is much stronger than that in LiNiO_2 [19]. In the meantime, the content of Ni^{4+} keeps increasing during this high voltage plateau, indicating that the change of the Ni states during the high voltage charging may be also due to the disproportional reactions of Ni^{3+} into $\text{Ni}^{2+}/\text{Ni}^{4+}$ [52], resulting in a 47% Ni^{2+} and 52% Ni^{4+} composition at the Ch-4.5 state. Quantitatively, the charge transfer by Ni redox per 1 mol NNMO can be calculated by total Ni valence change times Ni content (1/3) and are shown in Table S2. The results during charging and discharging are both 0.35 mol, which is only about a half of total Na^+ transfer amount.

Other than the new findings of the reductive behavior of Ni at high voltages, the Ni redox behavior and the inactive Mn (Mn remains Mn^{4+} in the 2.3–4.5 V range, as expected and detailed in SI section 1) are generally consistent with most previous reports [26,31,37,38]. However, our quantitative analysis reveals that TM redox cannot compensate all the Na deintercalation. We now switch to our central findings of this work on directly probing the ARR activities in the NNMO system.

The O-K edge XAS spectra in both TEY and TFY mode are shown in Fig. S3 just for reader's reference because they cannot provide conclusive evidence of ARR reactions due to the strong Mn/Ni-O hybridization [39]. mRIXS images of all the five electrodes are shown in Fig. 2a. Clearly, the characteristic feature of lattice oxidized oxygen around 523.7 eV emission energy, which has been found in ARR systems as well as oxidized oxygen references [23,24,39,45,53], start to emerge at 4.0 V and gets strong and clear at 4.5 V (red arrows in Fig. 2a). The feature disappears at the fully discharged state, indicating a reversible ARR activity in NNMO system.

As demonstrated previously [24,54], super partial fluorescence yield (sPFY) could be extracted from the mRIXS images for quantitative analysis of the reversibility and relative contributions of ARR reactions, as shown in Fig. 2b. The intensity around 531 eV (pink shaded area) increases upon charging and forms a defined peak at Ch-4.2 and Ch-4.5, then completely recovers at discharged D-2.3 state. Fig. 2c displays the integrated peak areas of the shaded zone with the area of the pristine sample set to zero for comparison purpose. The evolution of the mRIXS images and sPFY analysis reveal directly the highly reversible ARR activity in the NNMO system. Note that the oxidation state of oxygen increases faster than Na^+ deintercalation amount increase from Ch-4.0 to Ch-4.5 (the points in x axis are according to specific capacity). This indicates again the reductive coupling mechanism, as discussed above, leads to electron transfers from oxygen anions to TM cations [51].

The combination of the O-K mRIXS-sPFY and Ni-L XAS analysis provide the ultimate interpretation of the redox mechanism of NNMO during the initial charge and discharge operation. The detailed

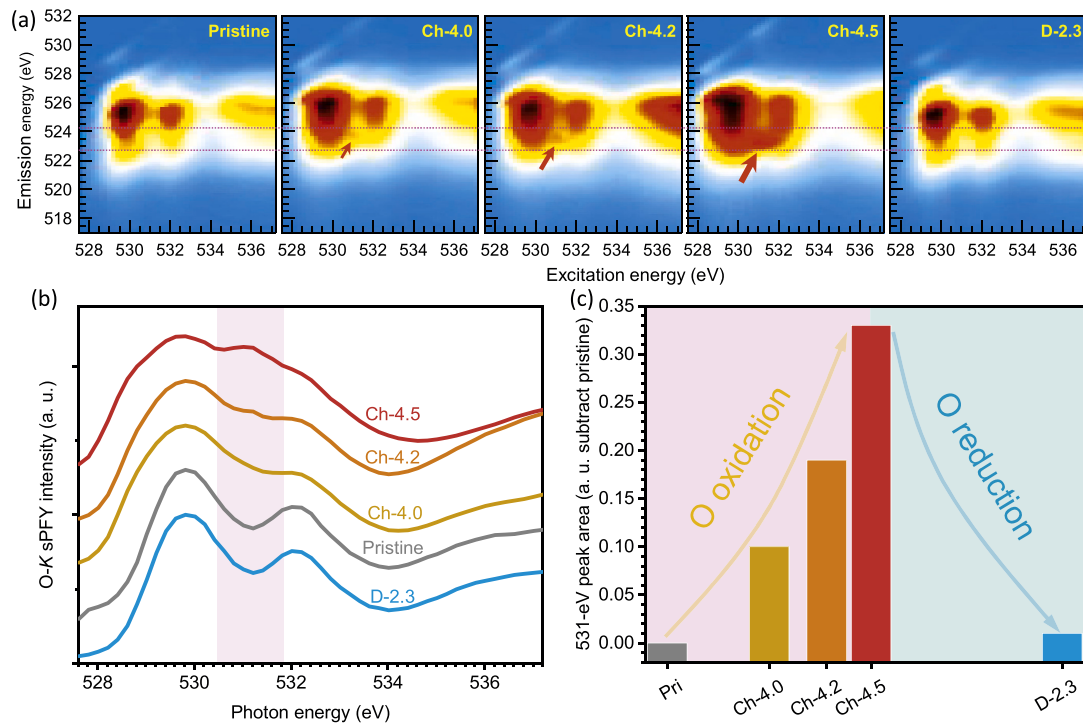


Fig. 2. The oxygen activities of $\text{Na}_{2/3}\text{Ni}_{1/3}\text{Mn}_{2/3}\text{O}_2$ during initial cycle. (a) The mRIXS images of $\text{Na}_{2/3}\text{Ni}_{1/3}\text{Mn}_{2/3}\text{O}_2$ electrodes. The key oxygen redox features are indicated by the red arrows. (b) The mRIXS-sPFY spectra extracted from mRIXS by integrating the characteristic 523.7 eV emission energy range, as indicated by the two horizontal dashed lines in Fig. 2a. (c) The mRIXS-sPFY 531 eV peak areas.

description of the mRIXS-sPFY quantification is provided in [Supplementary Information Section 1](#) and has been demonstrated in previous works [24,54]. [Table S2](#) and [Fig. 3](#) show the quantitative analysis results of the Ni and O redox in different stages marked with different colors. The charge transfer of ARR in stage 1, 2 and 3 are 0.08, 0.18 and 0.25 mol, respectively. Thus, the reversibility of ARR in the initial cycle is $0.25/(0.08 + 0.18) = 96\%$. Note this value of reversibility depends only on the relative mRIXS feature change at charged and discharged state, independent of the absolute quantification numbers. The grey area in stage 2 (0.04 mol) has to be from irreversible reactions, including surface oxygen activity and other interface reactions [19,54,55]. Other than this small amount of contributions from irreversible reactions, the

spectral analysis results of the ARR and Ni redox contributions are in excellent agreement with electrochemical capacity.

4. Discussion and summary

The comprehensive spectroscopic studies of both the TM and O redox activities consistently show that reversible ARR strongly contribute to the charging and discharging process of $\text{Na}_{2/3}\text{Ni}_{1/3}\text{Mn}_{2/3}\text{O}_2$, especially during the 4.2V charging plateau. This finding is nontrivial because the system consists of only 3d transition metal elements and displays a negligible 0.1 V voltage hysteresis of the high voltage plateau, where ARR clearly takes place. Additionally, the excellent rate performance and cycling stability of our material indicating an optimum configuration of the ARR on its kinetics [34]. This is the first time that strong and reversible (96%) ARR is conclusively confirmed with highly reversible electrochemical profile in both the voltages and profile lineshape, which were previously considered inherent to only cationic redox reactions.

The results here trigger several intriguing questions. First, $\text{Na}_{2/3}\text{Ni}_{1/3}\text{Mn}_{2/3}\text{O}_2$ is a conventional system with only 3d TMs in the TM-O layer. This is fundamentally different from the other $\text{Na} = 2/3$ compounds with Li or Mg in the TM layer that were reported before with strong ARR [24,25,54], because the highly ionic bonding between Li/Mg and O resembles that in Li-rich systems. As a truly non-Na-rich system, the stoichiometry of the NNMO system does not “require” ARR to compensate for the charge transfer during cycling because Ni redox could nominally compensate all Na deintercalation. Therefore, the finding of clear signature of ARR in NNMO suggests that ARR does not rely on either the exhaustion of cationic redox reactions for charge transfer compensation or the alkali-rich environment.

Second, the independent probes of the TM redox and ARR show that the two redox reactions are mixed even during the high voltage charging. It remains unknown at this time whether such mixed activities help stabilize the ARR and/or improve its kinetics, nonetheless, such a behavior is in sharp contrast with most other ARR systems, including the

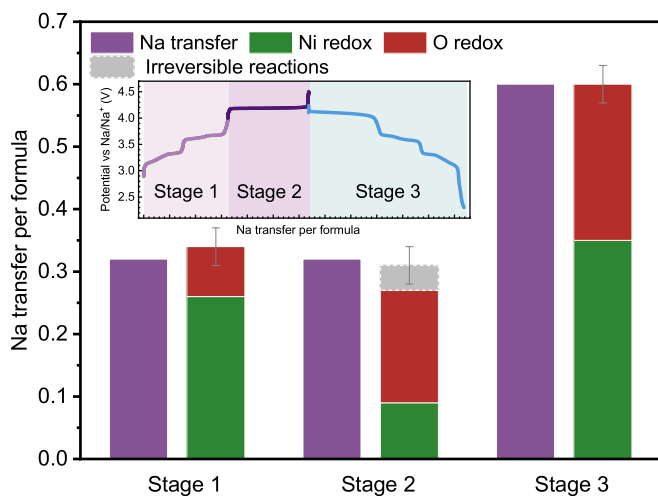


Fig. 3. Decipher the total electrochemical capacity by independent quantifications of Ni, Mn and O redox. The error bars represent the estimated total error of the three kinds of redox.

Li-rich and $\text{Na}_{2/3}\text{Mg}_{1/3}\text{Mn}_{2/3}\text{O}_2$ systems where ARR takes place exclusively at the high voltage during the initial charging [24,25,53].

Therefore, the finding of ARR in NNMO with a superior cycling performance not only provides the optimism on ARR system with good kinetics in conventional 3d TM materials, more importantly, it clarifies and detaches the seemingly inherent bounding between the ARR and kinetic issues. As an air-stable 3d TM material, our results suggest that NNMO is a unique candidate for studying the details of an optimized ARR system with the electrochemical performance comparable to established cationic redox systems. Further studies in both experiments and theory of such materials could lead to the developments of ARR-based commercially viable battery electrodes.

Declaration of competing interest

The authors declare that they have no known competing financial interests or personal relationships that could have appeared to influence the work reported in this paper.

CRediT authorship contribution statement

Kehua Dai: Conceptualization, Methodology, Investigation, Writing - original draft. **Jing Mao:** Investigation, Validation. **Zengqing Zhuo:** Investigation. **Yan Feng:** Validation. **Wenfeng Mao:** Validation. **Guo Ai:** Validation. **Feng Pan:** Validation. **Yi-de Chuang:** Methodology. **Gao Liu:** Supervision. **Wanli Yang:** Supervision, Conceptualization, Writing - review & editing.

Acknowledgment

We acknowledge the support from the National Natural Science Foundation of China (51604244), Postdoctoral research grant in Henan province (001802003), Science and Technology on Reliability Physics and Application of Electronic Component Laboratory open fund (ZHD201605) and Assistant Secretary for Energy Efficiency and Renewal Energy under the Battery Materials Research (BMR) program under Contract No. DE-AC02-05CH11231. Spectroscopic experiments were performed at the Advanced Light Source, a DOE Office of Science User Facility under contract no. DE-AC02-05CH11231.

Appendix A. Supplementary data

Supplementary data to this article can be found online at <https://doi.org/10.1016/j.nanoen.2020.104831>.

References

- P.K. Nayak, E.M. Erickson, F. Schipper, T.R. Penki, N. Munichandraiah, P. Adelhelm, H. Sclar, F. Amalraj, B. Markovsky, D. Aurbach, Review on challenges and recent advances in the electrochemical performance of high capacity Li- and Mn-rich cathode materials for Li-ion batteries, *Adv. Energy Mater.* 8 (2018), <https://doi.org/10.1002/aenm.201702397>.
- G. Assat, J.M. Tarascon, Fundamental understanding and practical challenges of anionic redox activity in Li-ion batteries, *Nat. Energy* 3 (2018) 373–386, <https://doi.org/10.1038/s41560-018-0097-0>.
- B. Li, D. Xia, Anionic redox in rechargeable lithium batteries, *Adv. Mater.* 29 (2017), <https://doi.org/10.1002/adma.201701054>.
- A. Grimaud, W.T. Hong, Y. Shao-Horn, J.M. Tarascon, Anionic redox processes for electrochemical devices, *Nat. Mater.* 15 (2016) 121–126, <https://doi.org/10.1038/nmat4551>.
- E. McCalla, A.M. Abakumov, M. Saubanère, D. Foix, E.J. Berg, G. Rousse, M.-L. Doublet, D. Gonbeau, P. Novák, G. Van Tendeloo, Visualization of OO peroxo-like dimers in high-capacity layered oxides for Li-ion batteries, *Science* 350 (2015) 1516–1521, <https://doi.org/10.1126/science.aac8260>.
- W. Yang, Oxygen release and oxygen redox, *Nat. Energy* 3 (2018) 619–620, <https://doi.org/10.1038/s41560-018-0222-0>.
- H. Konishi, T. Hirano, D. Takamatsu, A. Gunji, X.L. Feng, S. Furutsuki, Origin of hysteresis between charge and discharge processes in lithium-rich layer-structured cathode material for lithium-ion battery, *J. Power Sources* 298 (2015) 144–149, <https://doi.org/10.1016/j.jpowsour.2015.08.056>.
- K.G. Gallagher, J.R. Croy, M. Balasubramanian, M. Bettge, D.P. Abraham, A. K. Burrell, M.M. Thackeray, Correlating hysteresis and voltage fade in lithium- and manganese-rich layered transition-metal oxide electrodes, *Electrochim. Commun.* 33 (2013) 96–98, <https://doi.org/10.1016/j.elecom.2013.04.022>.
- J.R. Croy, K.G. Gallagher, M. Balasubramanian, Z. Chen, Y. Ren, D. Kim, S.-H. Kang, D.W. Dees, M.M. Thackeray, Examining hysteresis in composite $x\text{Li}_2\text{MnO}_3\text{(}1-x\text{)}\text{LiMO}_2$ cathode structures, *J. Phys. Chem. C* 117 (2013) 6525–6536, <https://doi.org/10.1021/jp312658q>.
- H.J. Yu, H.S. Zhou, Initial Coulombic efficiency improvement of the $\text{Li}_{1.2}\text{Mn}_{0.56}\text{Ni}_{0.16}\text{Co}_{0.06}\text{O}_2$ lithium-rich material by ruthenium substitution for manganese, *J. Mater. Chem.* 22 (2012) 15507–15510, <https://doi.org/10.1039/c2jm33484d>.
- H. Xu, S. Guo, H. Zhou, Review on anionic redox in sodium-ion batteries, *J. Mater. Chem. A* 7 (2019) 23662–23678, <https://doi.org/10.1039/C9TA06389G>.
- A.R. Armstrong, M. Holzapfel, P. Novák, C.S. Johnson, S.-H. Kang, M. M. Thackeray, P.G. Bruce, Demonstrating oxygen loss and associated structural reorganization in the lithium battery cathode $\text{Li}[\text{Ni}_{0.2}\text{Li}_{0.2}\text{Mn}_{0.6}\text{O}_2]$, *J. Am. Chem. Soc.* 128 (2006) 8694–8698, <https://doi.org/10.1021/ja062027+>.
- A.R. Armstrong, P.G. Bruce, Electrochemistry beyond Mn^{4+} in $\text{Li}_{x}\text{Mn}_{1-y}\text{Li}_y\text{O}_2$, *Electrochim. Solid State Lett.* 7 (2004) A1–A4, <https://doi.org/10.1149/1.1625591>.
- P.E. Pearce, A.J. Perez, G. Rousse, M. Saubanère, D. Batuk, D. Foix, E. McCalla, A. M. Abakumov, G. Van Tendeloo, M.L. Doublet, J.M. Tarascon, Evidence for anionic redox activity in a tridimensional-ordered Li-rich positive electrode beta- Li_2IrO_3 , *Nat. Mater.* 16 (2017) 580–586, <https://doi.org/10.1038/nmat4864>.
- A.J. Perez, D. Batuk, M. Saubanère, G. Rousse, D. Foix, E. McCalla, E.J. Berg, R. Dugas, K.H.W. van den Bos, M.-L. Doublet, D. Gonbeau, A.M. Abakumov, G. Van Tendeloo, J.-M. Tarascon, Strong oxygen participation in the redox governing the structural and electrochemical properties of Na-rich layered oxide Na_2IrO_3 , *Chem. Mater.* 28 (2016) 8278–8288, <https://doi.org/10.1021/acs.chemmater.6b03338>.
- P. Rozier, M. Sathiya, A.-R. Paulraj, D. Foix, T. Desaunay, P.-L. Taberna, P. Simon, J.-M. Tarascon, Anionic redox chemistry in Na-rich $\text{Na}_2\text{Ru}_{1-y}\text{Sn}_y\text{O}_3$ positive electrode material for Na-ion batteries, *Electrochim. Commun.* 53 (2015) 29–32, <https://doi.org/10.1016/j.elecom.2015.02.001>.
- M. Sathiya, K. Ramesha, G. Rousse, D. Foix, D. Gonbeau, A.S. Prakash, M. L. Doublet, K. Hemalatha, J.M. Tarascon, High performance $\text{Li}_2\text{Ru}_{1-y}\text{Mn}_y\text{O}_3$ ($0.2 \leq y \leq 0.8$) cathode materials for rechargeable lithium-ion batteries: their understanding, *Chem. Mater.* 25 (2013) 1121–1131, <https://doi.org/10.1021/cm400193m>.
- J. Hong, W.E. Gent, P. Xiao, K. Lim, D.H. Seo, J. Wu, P.M. Csernica, C.J. Takacs, D. Nordlund, C.J. Sun, K.H. Stone, D. Passarello, W. Yang, D. Prendergast, G. Ceder, M.F. Toney, W.C. Chueh, Metal-oxygen decoordination stabilizes anion redox in Li-rich oxides, *Nat. Mater.* 18 (2019) 256–265, <https://doi.org/10.1038/s41563-018-0276-1>.
- N. Li, S. Sallis, J.K. Papp, J. Wei, B.D. McCloskey, W. Yang, W. Tong, Unraveling the cationic and anionic redox reactions in a conventional layered oxide cathode, *ACS Energy Lett.* 4 (2019) 2836–2842, <https://doi.org/10.1021/acsenergylett.9b02147>.
- Z.W. Lebens-Higgins, N.V. Faenza, M.D. Radin, H. Liu, S. Sallis, J. Rana, J. Vinckeviciute, P.J. Reeves, M.J. Zuba, F. Badway, N. Pereira, K.W. Chapman, T.-L. Lee, T. Wu, C.P. Grey, B.C. Melot, A. Van Der Ven, G.G. Amatucci, W. Yang, L.F. J. Piper, Revisiting the charge compensation mechanisms in $\text{LiNi}_{0.8}\text{Co}_{0.2-y}\text{Al}_y\text{O}_2$ systems, *Mater. Horiz.* (2019), <https://doi.org/10.1039/c9mh00765b>.
- J.-N. Zhang, Q. Li, C. Ouyang, X. Yu, M. Ge, X. Huang, E. Hu, C. Ma, S. Li, R. Xiao, W. Yang, Y. Chu, Y. Liu, H. Yu, X.-Q. Yang, X. Huang, L. Chen, H. Li, Trace doping of multiple elements enables stable battery cycling of LiCoO_2 at 4.6 V, *Nat. Energy* 4 (2019) 594–603, <https://doi.org/10.1038/s41560-019-0409-z>.
- G.-H. Lee, J. Wu, D. Kim, K. Cho, M. Cho, W. Yang, Y.-M. Kang, Reversible anionic redox activities in conventional $\text{LiNi}_{1/3}\text{Co}_{1/3}\text{Mn}_{1/3}\text{O}_2$ cathodes, *Angew. Chem. Int. Ed.* (2020), <https://doi.org/10.1002/anie.202001349>.
- W. Yang, T.P. Devereaux, Anionic and cationic redox and interfaces in batteries: advances from soft X-ray absorption spectroscopy to resonant inelastic scattering, *J. Power Sources* 389 (2018) 188–197, <https://doi.org/10.1016/j.jpowsour.2018.04.018>.
- K. Dai, J. Wu, Z. Zhuo, Q. Li, S. Sallis, J. Mao, G. Ai, C. Sun, Z. Li, W.E. Gent, W. C. Chueh, Y.-d. Chuang, R. Zeng, Z.-x. Shen, F. Pan, S. Yan, L.F.J. Piper, Z. Hussain, G. Liu, W. Yang, High reversibility of lattice oxygen redox quantified by direct bulk probes of both anionic and cationic redox reactions, *Joule* 3 (2019) 518–541, <https://doi.org/10.1016/j.joule.2018.11.014>.
- U. Maitra, R.A. House, J.W. Somerville, N. Tapia-Ruiz, J.G. Lozano, N. Guerrini, R. Hao, K. Luo, L. Jin, M.A. Perez-Osorio, F. Massel, D.M. Pickup, S. Ramos, X. Lu, D.E. McNally, A.V. Chadwick, F. Giustino, T. Schmitt, L.C. Duda, M.R. Roberts, P. G. Bruce, Oxygen redox chemistry without excess alkali-metal ions in $\text{Na}_{2/3}\text{Mg}_{0.28}\text{Mn}_{0.72}\text{O}_2$, *Nat. Chem.* 10 (2018) 288–295, <https://doi.org/10.1038/nchem.2923>.
- B. Mortemard de Boisse, S.-i. Nishimura, E. Watanabe, L. Lander, A. Tsuchimoto, J. Kikkawa, E. Kobayashi, D. Asakura, M. Okubo, A. Yamada, Highly reversible oxygen-redox chemistry at 4.1 V in $\text{Na}_{4/7-x}\square_{1/7}\text{Mn}_{6/7}\text{O}_2$ (\square : Mn vacancy), *Adv. Energy Mater.* 8 (2018), <https://doi.org/10.1002/aenm.201800409>.
- B.H. Song, M.X. Tang, E.Y. Hu, O.J. Borkiewicz, K.M. Wiaderek, Y.M. Zhang, N. D. Phillip, X.M. Liu, Z. Shadique, C. Li, L.K. Song, Y.Y. Hu, M.F. Chi, G.M. Veith, X. Q. Yang, J. Liu, J. Nanda, K. Page, A. Huq, Understanding the low-voltage hysteresis of anionic redox in $\text{Na}_2\text{Mn}_3\text{O}_7$, *Chem. Mater.* 31 (2019) 3756–3765, <https://doi.org/10.1021/acs.chemmater.9b00772>.
- X. Rong, J. Liu, E. Hu, Y. Liu, Y. Wang, J. Wu, X. Yu, K. Page, Y.-S. Hu, W. Yang, H. Li, X.-Q. Yang, L. Chen, X. Huang, Structure-induced reversible anionic redox activity in Na layered oxide cathode, *Joule* 2 (2018) 125–140, <https://doi.org/10.1016/j.joule.2017.10.008>.

[29] R.A. House, U. Maitra, M.A. Pérez-Osorio, J.G. Lozano, L. Jin, J.W. Somerville, L. C. Duda, A. Nag, A. Walters, K. Zhou, M.R. Roberts, P.G. Bruce, Superstructure control of first-cycle voltage hysteresis in O-redox cathodes, *Nature* (2019), <https://doi.org/10.1038/s41586-019-1854-3>.

[30] Z. Lu, J.R. Dahn, In situ X-ray diffraction study of P2-Na_{2/3}[Ni_{1/3}Mn_{2/3}]O₂, *J. Electrochem. Soc.* 148 (2001) A1225–A1229, <https://doi.org/10.1149/1.1407247>.

[31] D.H. Lee, J. Xu, Y.S. Meng, An advanced cathode for Na-ion batteries with high rate and excellent structural stability, *Phys. Chem. Chem. Phys.* 15 (2013) 3304–3312, <https://doi.org/10.1039/c2cp4467d>.

[32] H. Wang, B. Yang, X.-Z. Liao, J. Xu, D. Yang, Y.-S. He, Z.-F. Ma, Electrochemical properties of P2-Na_{2/3}[Ni_{1/3}Mn_{2/3}]O₂ cathode material for sodium ion batteries when cycled in different voltage ranges, *Electrochim. Acta* 113 (2013) 200–204, <https://doi.org/10.1016/j.electacta.2013.09.098>.

[33] R. Qiao, Y. Wang, P. Olalde-Velasco, H. Li, Y.-S. Hu, W. Yang, Direct evidence of gradient Mn(II) evolution at charged states in LiNi_{0.5}Mn_{1.5}O₄ electrodes with capacity fading, *J. Power Sources* 273 (2015) 1120–1126, <https://doi.org/10.1016/j.jpowsour.2014.10.013>.

[34] J. Mao, X. Liu, J. Liu, H. Jiang, T. Zhang, G. Shao, G. Ai, W. Mao, Y. Feng, W. Yang, G. Liu, K. Dai, P2-type Na_{2/3}Ni_{1/3}Mn_{2/3}O₂ cathode material with excellent rate and cycling performance for sodium-ion batteries, *J. Electrochem. Soc.* 166 (2019) A3980–A3986, <https://doi.org/10.1149/2.0211916jes>.

[35] T. Risthaus, D. Zhou, X. Cao, X. He, B. Qiu, J. Wang, L. Zhang, Z.P. Liu, E. Paillard, G. Schumacher, M. Winter, J. Li, A high-capacity P2 Na_{2/3}Ni_{1/3}Mn_{2/3}O₂ cathode material for sodium ion batteries with oxygen activity, *J. Power Sources* 395 (2018) 16–24, <https://doi.org/10.1016/j.jpowsour.2018.05.026>.

[36] C. Cheng, S. Li, T. Liu, Y. Xia, L.Y. Chang, Y. Yan, M. Ding, Y. Hu, J. Wu, J. Guo, L. Zhang, Elucidation of anionic and cationic redox reactions in a prototype sodium-layered oxide cathode, *ACS Appl. Mater. Interfaces* 11 (2019) 41304–41312, <https://doi.org/10.1021/acsami.9b13013>.

[37] C. Ma, J. Alvarado, J. Xu, R.J. Clement, M. Kodur, W. Tong, C.P. Grey, Y.S. Meng, Exploring oxygen activity in the high energy P2-type Na_{0.78}Ni_{0.23}Mn_{0.69}O₂ cathode material for Na-Ion batteries, *J. Am. Chem. Soc.* 139 (2017) 4835–4845, <https://doi.org/10.1021/jacs.7b00164>.

[38] X. Wu, G.-L. Xu, G. Zhong, Z. Gong, M.J. McDonald, S. Zheng, R. Fu, Z. Chen, K. Amine, Y. Yang, Insights into the effects of zinc doping on structural phase transition of P2-type sodium nickel manganese oxide cathodes for high-energy sodium ion batteries, *ACS Appl. Mater. Interfaces* 8 (2016) 22227–22237, <https://doi.org/10.1021/acsami.6b06701>.

[39] Q. Ruimin, R. Subhayan, Z. Zengqing, L. Qinghao, L. Yingchun, K. Jung-Hyun, L. Jun, L. Eungie, P. Bryant, G. Jinghua, Y. Shishen, H. Yongsheng, L. Hong, P. David, Y. Wanli, Deciphering the Oxygen Absorption Pre-edge: Universal Map of Transition Metal Redox Potentials in Batteries, 2019, <https://doi.org/10.26434/chemrxiv.11416374.v2>.

[40] Q.H. Li, R.M. Qiao, L.A. Wray, J. Chen, Z.Q. Zhuo, Y.X. Chen, S.S. Yan, F. Pan, Z. Hussain, W.L. Yang, Quantitative probe of the transition metal redox in battery electrodes through soft x-ray absorption spectroscopy, *J. Phys. D Appl. Phys.* 49 (2016) 413003, <https://doi.org/10.1088/0022-3727/49/41/413003>.

[41] R.M. Qiao, L.A. Wray, J.H. Kim, N.P.W. Pieczonka, S.J. Harris, W.L. Yang, Direct experimental probe of the Ni(II)/Ni(III)/Ni(IV) redox evolution in LiNi_{0.5}Mn_{1.5}O₄ electrodes, *J. Phys. Chem. C* 119 (2015) 27228–27233, <https://doi.org/10.1021/acs.jpcc.5b07479>.

[42] R.M. Qiao, Y.S. Wang, P. Olalde-Velasco, H. Li, Y.S. Hu, W.L. Yang, Direct evidence of gradient Mn(II) evolution at charged states in LiNi_{0.5}Mn_{1.5}O₄ electrodes with capacity fading, *J. Power Sources* 273 (2015) 1120–1126, <https://doi.org/10.1016/j.jpowsour.2014.10.013>.

[43] R.M. Qiao, K.H. Dai, J. Mao, T.C. Weng, D. Sokaras, D. Nordlund, X.Y. Song, V. S. Battaglia, Z. Hussain, G. Liu, W.L. Yang, Revealing and suppressing surface Mn(II) formation of Na_{0.44}MnO₂ electrodes for Na-ion batteries, *Nano Energy* 16 (2015) 186–195, <https://doi.org/10.1016/j.nanoen.2015.06.024>.

[44] J. Wu, Q. Li, S. Sallis, Z. Zhuo, W.E. Gent, W.C. Chueh, S. Yan, Y.-d. Chuang, W. Yang, Fingerprint oxygen redox reactions in batteries through high-efficiency mapping of resonant inelastic X-ray scattering, *Condensed Matter* (2019) 4, <https://doi.org/10.3390/condmat4010005>.

[45] Z. Zhuo, C.D. Pemmaraju, J. Vinson, C. Jia, B. Moritz, I. Lee, S. Sallis, Q. Li, J. Wu, K. Dai, Y.D. Chuang, Z. Hussain, F. Pan, T.P. Devereaux, W. Yang, Spectroscopic signature of oxidized oxygen states in peroxides, *J. Phys. Chem. Lett.* 9 (2018) 6378–6384, <https://doi.org/10.1021/acs.jpcllett.8b02757>.

[46] R. Qiao, Q. Li, Z. Zhuo, S. Sallis, O. Fuchs, M. Blum, L. Weinhardt, C. Heske, J. Pepper, M. Jones, A. Brown, A. Spucces, K. Chow, B. Smith, P.-A. Glans, Y. Chen, S. Yan, F. Pan, L.F.J. Piper, J. Denlinger, J. Guo, Z. Hussain, Y.-D. Chuang, W. Yang, High-efficiency in situ resonant inelastic X-ray scattering (IRIXS) endstation at the Advanced Light Source, *Rev. Sci. Instrum.* 88 (2017), 033106, <https://doi.org/10.1063/1.4977592>.

[47] Y.-D. Chuang, Y.-C. Shao, A. Cruz, K. Hanzel, A. Brown, A. Frano, R. Qiao, B. Smith, E. Domning, S.-W. Huang, L.A. Wray, W.-S. Lee, Z.-X. Shen, T.P. Devereaux, J.-W. Chiou, W.-F. Pong, V.V. Yashchuk, E. Gullikson, R. Reininger, W. Yang, J. Guo, R. Duarte, Z. Hussain, Modular soft x-ray spectrometer for applications in energy sciences and quantum materials, *Rev. Sci. Instrum.* 88 (2017), 013110, <https://doi.org/10.1063/1.4974356>.

[48] J. Wu, S. Sallis, R. Qiao, Q. Li, Z. Zhuo, K. Dai, Z. Guo, W. Yang, Elemental-sensitive detection of the chemistry in batteries through soft x-ray absorption spectroscopy and resonant inelastic x-ray scattering, *J. Vis. Exp.* 134 (2018), e57415, <https://doi.org/10.3791/57415>.

[49] M. Saubanère, E. McCalla, J.-M. Tarascon, M.-L. Doublet, The intriguing question of anionic redox in high-energy density cathodes for Li-ion batteries, *Energy Environ. Sci.* 9 (2016) 984–991, <https://doi.org/10.1039/C5EE03048J>.

[50] M. Sathiya, G. Rousse, K. Ramesha, C.P. Laiqa, H. Vezin, M.T. Sougrati, M. L. Doublet, D. Foix, D. Gonbeau, W. Walker, A.S. Prakash, M. Ben Hassine, L. Dupont, J.M. Tarascon, Reversible anionic redox chemistry in high-capacity layered-oxide electrodes, *Nat. Mater.* 12 (2013) 827–835, <https://doi.org/10.1038/nmat3699>.

[51] E.J. Kim, L.A. Ma, L.C. Duda, D.M. Pickup, A.V. Chadwick, R. Younesi, J.T. S. Irvine, A.R. Armstrong, Oxygen redox activity through a reductive coupling mechanism in the P3-type nickel-doped sodium manganese oxide, *ACS Appl. Energy Mater.* (2019), <https://doi.org/10.1021/acsaem.9b02171>.

[52] H. Chen, C.L. Freeman, J.H. Harding, Charge disproportionation and Jahn-Teller distortion in LiNiO₂ and NaNiO₂: a density functional theory study, *Phys. Rev. B* 84 (2011), 085108, <https://doi.org/10.1103/PhysRevB.84.085108>.

[53] J. Xu, M. Sun, R. Qiao, S.E. Renfrew, L. Ma, T. Wu, S. Hwang, D. Nordlund, D. Su, K. Amine, J. Lu, B.D. McCloskey, W. Yang, W. Tong, Elucidating anionic oxygen activity in lithium-rich layered oxides, *Nat. Commun.* 9 (2018) 947, <https://doi.org/10.1038/s41467-018-03403-9>.

[54] J. Wu, Z. Zhuo, X. Rong, K. Dai, Z. Lebens-Higgins, S. Sallis, F. Pan, L.F.J. Piper, G. Liu, Y.-d. Chuang, Z. Hussain, Q. Li, R. Zeng, Z.-x. Shen, W. Yang, Dissociate lattice oxygen redox reactions from capacity and voltage drops of battery electrodes, *Sci. Adv.* 6 (2020), <https://doi.org/10.1126/sciadv.aaw3871>.

[55] Q.N. Liu, Z. Hu, M.Z. Chen, C. Zou, H.L. Jin, S. Wang, Q.F. Gu, S.L. Chou, P2-type Na_{2/3}Ni_{1/3}Mn_{2/3}O₂ as a cathode material with high-rate and long-life for sodium ion storage, *J. Mater. Chem. A* 7 (2019) 9215–9221, <https://doi.org/10.1039/c8ta11927a>.



Dr. Kehua Dai received his Ph.D. and bachelor's degree in Applied Chemistry from Peking University in 2008. From 2008 to 2019, he worked in Northeastern University, China. Currently he works in the College of Chemistry, Tianjin Normal University as an associate professor from 2020. His research interests focus mainly on high energy electrode materials and core-level X-ray spectroscopy.



Dr. Jing Mao received her Ph.D. in Physical Chemistry of Metallurgy from Northeastern University in 2013. Currently, she is a faculty at School of Materials Science and Engineering, Zhengzhou University, China. Her research interests focus mainly on developing high energy electrode cathode materials, modelling and safety for lithium ion batteries.



Dr. Zengqing Zhuo received the B.S. degree in 2013 and the Ph.D. degree in 2019 from Peking University, China. He is currently a postdoctoral researcher in Peking University, China. His main research field is soft x-ray spectroscopy for energy materials.



Dr. Yan Feng is an associate professor of College of Chemistry, Tianjin Normal University. She received her Ph.D. degree of Inorganic Chemistry from Nankai University in 2007. After two-year postdoctoral training in Tianjin University, she joined Tianjin Normal University in 2009. She also worked as a visiting guest scientist in Lawrence Berkeley National Laboratory from 2014 to 2016, and 2018. Her research focuses on preparation and electrochemical performances of cathode and anode materials of lithium-ion batteries and lithium-sulfur batteries.



Dr. Yi-De Chuang is a staff scientist at the Advanced Light Source (ALS), Lawrence Berkeley National Laboratory. He received his Ph.D. degree in Physics from the University of Colorado at Boulder in 2001. He worked as an ALS postdoctoral fellow after graduation and became an ALS staff in 2006. His research focus is on using soft x-ray spectroscopies to study the materials' electronic structures and also developing novel soft x-ray instrumentation to advance these spectroscopies.



Dr. Wenfeng Mao received his Ph.D. in Applied chemistry at Tianjin University in 2016. From 2016 to 2019, he worked in GAC Automotive Research & Development Center, China. He joined the College of Chemistry at Tianjin Normal University as an assistant professor in 2019. His research interest focuses on the syntheses and properties of new materials for energy storage devices.



Dr. Gao Liu is a Staff Scientist and Principal Investigator in Energy Technologies Area at Lawrence Berkeley National Laboratory, specialized in lithium battery research. Since he joined Lawrence Berkeley Lab in 2001, Dr. Liu has led energy storage R&D projects for the Department of Energy and industries, and developed key technologies including conductive binders and application of lithium metal to improve battery performance. He has also collaborated with companies to commercialize new battery technologies. He has received numerous awards including R&D100 Award in 2013 and FMC Scientific Achievement Award in 2014.



Dr. Guo Ai received her Ph.D. degree from Beijing University, China in 2012. From 2012 to 2018, she worked in No. 5 Electronic Research Institute of the Ministry of Industry and Information Technology, Guangzhou. She is now a professor in College of Physics and Materials Science at Tianjin Normal University. Her research field is the energy material synthesis and application for energy storage devices.



Dr. Wanli Yang is a staff scientist at the Advanced Light Source of Lawrence Berkeley National Laboratory. His research interest focuses on soft x-ray spectroscopy of electrochemical materials. He has recently led the efforts on introducing resonant inelastic x-ray scattering (RIXS) as a powerful technique for practical material researches, especially for detecting the evolving chemical states of both transition metals and oxygen in battery electrodes.



Dr. Feng Pan, founding Dean of School of Advanced Materials, Peking University Shenzhen Graduate School, got B. S. from Dept. Chemistry, Peking University in 1985 and Ph.D. from Dept. of P&A Chemistry, University of Strathclyde, Glasgow, UK, with "Patrick D. Ritchie Prize" for the best Ph.D. in 1994. With more than a decade experience in large international incorporations, Prof. Pan has been engaged in fundamental research and product development of novel optoelectronic and energy storage materials and devices.